

## ON SIMULATION OF CLUSTER FORMATION PROCESS UNDER WATER VAPOR SPHERICAL EXPANSION INTO VACUUM

**N.Yu. Bykov**

Peter the Great St. Petersburg Polytechnic University, St. Petersburg, Russian Federation

The calculation of a water vapor outflow into vacuum has been performed using the direct simulation Monte Carlo with taking into account a condensation process. Two cluster-formation models were employed for simulation. The former is based on a kinetic approach, the latter is based on conclusions drawn from the modified classical nucleation theory. The analysis of physical adequacy of models and features of their program implementation was carried out. The simulation of spherical vapor expansion from an evaporating surface was performed over a range of Knudsen numbers corresponding to transient and near-continual flow regimes. The influence of a condensation process on gasdynamic flow parameters was analyzed. The effect of freezing of cluster mole-fractions when receding from the evaporating source was demonstrated.

**Key words:** direct simulation Monte Carlo; condensation; water cluster; transient flow regime

**Citation:** N.Yu. Bykov, On simulation of cluster formation process under water vapor spherical expansion into vacuum, St. Petersburg Polytechnical State University Journal. Physics and Mathematics. 11 (1) (2018) 37 – 49. DOI: 10.18721/JPM.11109

### Introduction

The processes of condensation of water vapor in expanding flows are widespread in nature and technology. Natural phenomena include atmospheric events such as water clusters developing in gas flows making up the near-nucleus atmosphere of comets [1]. Technical applications concern the processes of condensation of water vapor in nozzles and jets [2], for example, in spacecraft engines working at high altitudes [3].

Depending on the characteristic Knudsen number ( $Kn = \lambda/D$ , where  $\lambda$  is the mean free path of molecules, and  $D$  is the characteristic flow dimension), the outflow of vapor into vacuum is rarefied at the periphery of the jet or in the entire flow region. The direct simulation Monte Carlo method (DSMC) is traditionally used to calculate rarefied flows [4].

The interest towards modeling the formation and growth of clusters in rarefied flows by the DSMC method started in the early

2000s in connection with the rapidly evolving vacuum technologies for deposition of various coatings, including laser ablation technologies. These flows were calculated by kinetic models [5 – 8], where probabilities of particle association in mutual collisions were cluster size functions (equal to unity in the simplest case), and the monomolecular cluster decay was simulated by the formula of the Rice – Ramsperger – Kassel (RRK) theory. The studies gave a detailed description of the first stage of cluster formation (dimerization) and implemented the RRK formula for monomolecular decay algorithmically. The method of direct statistical modeling of flows with condensation processes based on the kinetic model was further developed in [9], where the probabilities of the association processes were obtained using the molecular dynamics (MD) approaches, and also in [10], which offered an exact algorithm for implementing the RRK formula for monomolecular decay for the DSMC method. It was found in all of these studies that the rates

of the forward process of particle association and the reverse process of decay were not related to each other. Ref. [11] proposed a condensation model where the probabilities of cluster growth/decay were obtained from the data on the rates of forward and reverse reactions of the corresponding processes. The rate constants of the forward and reverse reactions are related by the equilibrium constants which are assumed to be known. Distinctive aspects of [11] are the original expressions for the probability of monomolecular cluster decay (coinciding with the RRK theory in a particular case) and the probability of dimer formation in a three-particle collision of monomers. This kinetic model [11] was used for obtaining the key results of this paper.

Another group of studies [12, 13] described performing DSMC calculations of water vapor condensation in a rarefied far field of a jet engine plume. These papers used classical nucleation theory (CNT), with conclusions adapted for the DSMC algorithm.

The intention to employ CNT for practical calculations seems well-grounded. First of all, the theory's conclusions have long been used to describe flows with condensation. The required thermodynamic parameters (vapor pressure and temperature, supersaturation degree, nucleation rate and critical cluster size) can be calculated within the framework of DSMC. Secondly, simulation of the cluster growth process, starting from the formation of a critical nucleus, has its computational advantages, eliminating the need to spend the computational time on simulating the formation of subcritical clusters, including the formation of a dimer in triple recombination of monomers.

However, CNT also has its known drawbacks, as it uses the concept of surface tension for small clusters and predicts the size of the critical cluster to be less than unity for high values of vapor supersaturation. Refs. [12, 13] ignored the effect of the release of binding energy during particle association, and, consequently, failed to take into account the effect of increasing internal temperature of the cluster accompanying this process; the implementation of the algorithm for the case of high supersaturation was not clarified as well.

To eliminate these shortcomings of CNT, it

was proposed in [14] to use modified classical nucleation theory (MCNT). Within the MCNT model, there is no need to involve the concept of surface tension [15], and the size of the critical cluster for high supersaturation values is equal to unity. This latter circumstance entails making additional assumptions in the algorithmic implementation of the model. The MCNT model was implemented for the spatially homogeneous case of condensation of copper vapor [16]. However, a direct comparison of the calculation results obtained for the same flows using both models (based on the kinetic and the MCNT approach) has not been carried out. Additionally, comprehensive analysis of the algorithmic possibilities of implementing the MCNT model has not been performed for the DSMC method.

One of the goals of this study was to compare the results of calculations (we calculated the size distributions of the resulting clusters and the coordinate distributions of gasdynamic parameters) using the two models (kinetic and MCNT) with one object as an example.

The paper also discusses the specifics of algorithmic implementation of the MCNT approach and the parameters of the MCNT model for which these calculated results are close to the ones obtained by the kinetic approach.

The object chosen for study in the paper was a steady one-dimensional flow of water vapor from an evaporating spherical surface. Simulation of the expansion of non-reacting gas from the surface of a sphere into vacuum was performed in [17, 18]. These studies considered the effect of the degree of rarefaction on gas dynamics of the flow, analyzed the peculiarities of formation of the Knudsen layer near the surface of the sphere and the relaxation of translational degrees of freedom.

Ref. [19] calculated the parameters of clusters in the region  $X < 5R$  ( $X$  is the radial coordinate,  $R$  is the radius of the sphere) and of the vapor at the sonic line during the expansion of water vapor from a spherical source. A simplified condensation model was used for the calculations: in particular, the probabilities of particle association were assumed to be equal to unity during clustering reactions, and the evaporation process was simulated by the RRK



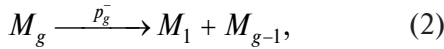
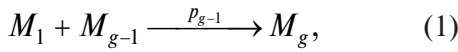
theory. A significant mass fraction of clusters (up to 19%) was observed within the flow field for the model parameters used in [19], and the condensation process was confirmed to have a considerable effect on the parameters of the sonic line.

Other goals of this paper were to carry out a series of calculations for flow from a spherical source using a refined condensation model proposed in [11], to study the effect of the clustering process on the parameters of vapor flow and to study the parameters of the forming clusters.

### Model of cluster formation

According to the data given in [11], a water cluster  $M_g$  is characterized by the number of monomers  $g$ , the number of surface monomers  $g_0$ , the mass  $m_g$ , the diameter  $d_g$ , the translational velocity  $\mathbf{v}_g$ , the internal energy  $E_{int,g}$ , the number of rotational ( $\zeta_{r,g}$ ) and vibrational ( $Z_{v,g}$ ) degrees of freedom and the energy of evaporation of one monomer from the surface  $\varepsilon_g$ .

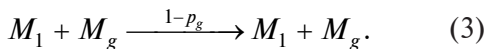
The following association/decay reactions are considered for clusters of size  $g > 2$ :



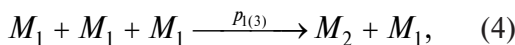
where  $p_{g-1}$ ,  $p_g^-$  are the probabilities of association and decay, respectively.

Reaction (1) describes the attachment of a monomer to a cluster in a binary collision, reaction (2) describes the unimolecular decay of the cluster. The unimolecular decay time of the cluster is of the order of  $1/\nu_0$ , where  $\nu_0$  is the characteristic vibrational frequency of the monomers in the cluster. The forward process (1) is characterized by the rate constant  $K_{g-1}$ , the inverse process (2) is characterized by the rate constant  $K_g^-$ .

An elastic collision between a monomer and a cluster occurs with the probability  $1-p_g$ :

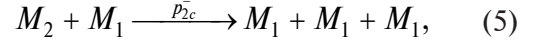


Within the framework of the model under consideration, water dimers are formed as a result of three-particle collisions:



where  $p_{1(3)}$  is the respective probability.

The reverse reaction occurs by the scheme:



where  $p_{2c}^-$  is the probability of collision decay.

Let us denote the rates of the forward (4) and the reverse (5) reactions by  $K_{1(3)}$  and  $K_{2c}^-$ , respectively.

### Model based on the modified classical nucleation theory

The specifics of the MCNT-based model is that the size of the critical cluster  $g_*$  and the nucleation rate  $J$ , which are functions of thermophysical parameters, have to be calculated in each computational cell.

Within the MCNT model, the nucleation rate is determined as follows [2, 15]:

$$J = 1 / \sum_{g=2}^{\infty} R_g^{-1}, \quad R_g = K_{g-1} n_1 n_{g-1}^e, \quad (6)$$

where  $n_g$  is the concentration of  $g$ -mers;  $K_{g-1}$  are the rate constants of processes (1) and (4) for  $g > 2$  (for the case when water dimers form through reaction (4),  $K_1 = K_{1(3)} n_1$ ); the superscript  $e$  denotes the equilibrium concentration,  $n_1^e = n_1$ .

A given degree of supersaturation  $S$  corresponds to a certain critical cluster size  $g_*$  [2, 15]. The critical size in the range  $S < S_{\min}$  is equal to the critical size determined according to classical nucleation theory (CNT) [2]; this size is equal to the coordination number  $N_c$  in the range  $S_{\min} < S < S_{\max}$ , while for the case  $S > S_{\max}$   $g_* = 1$ . The  $S_{\max}$  and  $S_{\min}$  values were determined in [14, 15]. The critical cluster size has to be found for determining the value of  $J$ , since clusters of near-critical size make the main contribution to the sum in expression (6).

After the values of  $J$  and  $g_*$  have been determined, the computational algorithm based on the MCNT approach is reduced to injecting clusters into a cell at a rate  $J$ . Determining the size of the injected clusters is the first distinctive feature of the MCNT-based algorithm. In [12, 13] clusters of critical size  $g_*$  were injected into the cell. Injecting clusters of size  $g_* > 2$  into a cell leads to a reduction of the real size distribution of the clusters. In this case it is assumed that

the concentrations of subcritical clusters in the cell correspond to the equilibrium distribution. In this situation, additional simulation of the distribution of subcritical clusters has to be carried out within the framework of the DSMC method (this problem was not considered in [12, 13]) and changes have to be made to the computational algorithm. On the other hand, with  $S \gg 1$ ,  $g_* = 1$  within the MCNT approach (classical nucleation theory predicts that  $g_* < 1$  for this case). There is no point in injecting monomers into the cell. Since the growth rates of clusters of any size within CNT are equal to the nucleation rates  $J$  [2], it is possible to inject clusters of near-critical or subcritical size  $g_a$  into the cell [14]. Choosing  $g_a = 2$  for the size of the cluster is optimal, since, on the one hand, the distribution of the clusters by size (starting with the dimer) should be reproduced in any cell, and on the other hand, this solves the problem of injecting clusters with  $S \gg 1$ . This is exactly the approach used in our study.

The second distinctive feature of the MCNT-based algorithm is that the reactions of growth of  $g_a$ -sized clusters (during the association of a monomer and a cluster of size  $(g_a - 1)$ ) and of their decay are excluded from the computational algorithm, as both processes are included in the nucleation rate  $J$  [2].

The third distinctive feature of the computational algorithm based on MCNT is that the vapor temperature has to be determined for performing Monte Carlo simulations of the evaporation process. In the standard case, it is not necessary to determine the macroscopic parameters at each time step for the purpose of simulating the collisions and motions of molecules by the DSMC method. Models based on MCNT or CNT are single-temperature, i.e., they assume that the translational and internal temperatures of monomers and clusters are equal. Since clustering leads to release of latent condensation heat into the flow, this approach implies using a single temperature to determine the rate constants of growth and decay of clusters. This can be either the translational monomer temperature  $T_1$ , or the temperature  $T_{tot}$ , averaged over the translational and internal energies of the particles in the cell [11]. On the one hand, however, if  $n_1 \gg n_g$ , the averaged temperature  $T_{tot}$  is close to the translational

monomer temperature  $T_1$ , and, the same as  $T_1$ , it does not reflect the real internal energy of the individual cluster  $g$ . On the other hand, the implementation of the algorithm using the  $T_{tot}$  quantity means that the changes that are incorrect from a physical standpoint have to be introduced to the main collision module of the program, since the number of collisions in a cell depends on temperature. In view of these circumstances, we have used the monomer temperature  $T_1$  to determine the reaction rates in this study.

We should note that it is possible to implement a mixed algorithm (this option is also considered in this paper) where dimers are injected into the flow field according to the MCNT algorithm, and the subsequent process of cluster evaporation is considered in a manner similar to the kinetic approach (the probability of a monomer evaporating from a cluster depends on the internal temperature of the individual cluster). However, this computational model cannot be accepted as correct from the standpoint of basic CNT.

### The kinetic approach to constructing the model

The kinetic approach involves no additional assumptions about the size of the clusters injected into the computational cell or about the calculation of the nucleation rate. Clustering starts with the formation of dimers by reaction (4).

The probabilities of the reactions occurring in case of known rate constants are determined using the Total Collision Energy model (TCE) [4, 20, 21]. This model is based on the assumption that the corresponding probabilities can be given in the form

$$p = L \frac{(E_{tot} - \varepsilon)^{Y + \zeta_{tot}/2 - 1}}{E_{tot}^{\zeta_{tot}/2 - 1}}, \quad (7)$$

where  $E_{tot}$  is the total energy;  $\zeta_{tot}$  is the total number of degrees of freedom;  $\varepsilon$  is the activation energy;  $L$ ,  $Y$  are the constants depending on the parameters of the model of elastic collisions of particles and the parameters of the rate constants of reactions.

To determine the parameters  $L$  and  $Y$  in expression (7), the reaction rate constants should be given in the Arrhenius form:





$$K = AT^B \exp(-\varepsilon/kT)$$

( $k$  is the Boltzmann constant); the constants  $A$ ,  $B$  and the activation energy  $\varepsilon$  are assumed to be known.

The kinetic model notably lacks the drawbacks of the MCNT model as it does not require either determining the macroscopic temperature in the cell or making additional assumptions about the size of the clusters injected into the cell and their parameters.

### Problem statement

The goal of this study is in calculating spherical steady-state expansion of water vapor from the surface of a sphere of radius  $R$  into vacuum. The calculation was performed using the direct simulation Monte Carlo method taking into account the process of vapor condensation in the volume.

The problem under consideration is one-dimensional, with a single radial coordinate  $X$ . However, implementing the DSMC method involves simulating all three components of particle velocity: the radial one  $v_x$  and the two components perpendicular to it,  $v_\theta$  and  $v_\phi$ . The source temperature  $T_0$  is assumed to be constant. Only monomers (molecules) of water evaporate from the surface. Evaporation is described by the Hertz – Knudsen law according to which the flux  $F^+$  of evaporating molecules is equal to

$$F^+ = n_0 v_0 / 4,$$

where  $n_0$  is the concentration of saturated vapor (corresponding to the equilibrium pressure determined by  $T_0$ );  $v_0$  is the average thermal velocity of the evaporating particles;

$$v_0 = (8kT_0/\pi m_1)^{1/2}$$

( $m_1$  is the monomer mass).

The equilibrium vapor pressure  $p_0(T)$  is determined in the same way as in [22]. The remaining parameters of water vapor correspond to those given in [23]. It is assumed that the distribution function for water molecules leaving the surface is semi-Maxwellian [19].

The vibrational degrees of freedom of the evaporating water molecules are assumed to be frozen for the range of source temperatures under consideration [24]. The internal energy of

the monomers leaving the surface is equal to the rotational energy

$$E_{int,1} = (\zeta_{r,1} / 2) k T_0.$$

The Larsen – Borgnakke model [4] is used for simulating the energy exchange between the translational and internal degrees of freedom. The probability of energy exchange between the rotational and translational degrees of freedom of water molecules in mutual collisions is taken equal to unity. The probabilities of energy exchange between the translational and internal degrees of freedom in monomer-cluster collisions are taken equal to 0.1 [10]. The formation of clusters in the flow field occurs according to the above-described condensation model. The reaction rate constants and the parameters of the collision models are taken from [25].

The molecules and clusters reaching the outer boundary of the region were excluded from the calculations (hypersonic boundary condition). The particles crossing the source boundary in the opposite direction were also excluded (the condition of total condensation on the surface).

The gas-dynamic flow pattern in the considered statement is determined by the Knudsen numbers

$$\text{Kn} = \lambda_0 / D = \lambda_0 / (2R),$$

where  $\lambda_0$  is the mean free path of the water molecules, corresponding to the parameters  $n_0$  and  $T_0$ ;  $D$  is the diameter of the sphere диаметр сферы, the characteristic reaction rates are given by (1), (2), (4), (5).

Calculation variants and the values of the determining parameters are listed in Table 1.

The calculations were performed by the DSCM method with a collision scheme without a time counter [4], using the developed software package at the Polytechnic RSC Tornado cluster of the Polytechnic University Supercomputer Center.

### Calculation results and discussion

Fig. 1 shows the simulation results, including data on the dynamics of the normalized values

Table 1

**Variants of calculation of spherical steady-state expansion of water vapor into vacuum**

Number	Model basis	Condensation taken into account	Knudsen number
1	–	–	$10^{-4}$
2	KA	+	$10^{-4}$
3	–	–	$10^{-2}$
4	KA	+	$10^{-2}$
5	MCNT	+	$10^{-4}$
6	MCNT + KA (for evaporation)	+	$10^{-4}$

Notes. 1. The source temperature was the same for all variants:  $T_0 = 350$  K. 2. The Knudsen number  $Kn = \lambda_0/(2R)$ , where  $\lambda_0$  is the mean free path,  $R$  is the radius of the sphere.

Abbreviations: MCNT stands for modified classical nucleation theory, KA stands for kinetic approach.

of the concentration, velocity, and temperature of the vapor in the flow field. The vapor density decreases with distance from the surface, asymptotically tending to zero, while the gas velocity increases (Fig. 1, *a*). In case of outflow into a continuous medium ( $Kn = 0$ ), the velocity tends to its thermodynamic limit of steady-state expansion

$$u = (2 / (\gamma - 1))^{1/2} a_0,$$

where  $\gamma$  is the adiabatic exponent;  $a_0$  is the sound velocity determined from the temperature  $T_0$  [26].

In case of collisionless expansion ( $Kn \rightarrow \infty$ ), the vapor velocity tends to the thermal velocity determined from the equilibrium vapor temperature on the surface [27]:

$$u_{\max} = v_0.$$

The heat content of the vapor drops to zero for continuous-medium flow [26].

The temperature of the gas in case of free-molecular flow drops to the value [27]:

$$T / T_0 = 1 - 8 / (3\pi)$$

(Fig. 1, *b*).

The decrease in the degree of flow rarefaction (a decrease in the Knudsen number) leads to a greater number of collisions between particles and a more efficient conversion of ther-

mal energy into the energy of directed motion of particles. As a result, the gas velocity for a more dense flow regime ( $Kn = 10^{-4}$ ) increases with respect to the more rarefied flow ( $Kn = 10^{-2}$ ), while the density and the temperature decrease with distance from the source.

Notably, the result indicates that increasing the Knudsen number leads to a violation of the equilibrium between the translational and the internal degrees of freedom [17, 18]. The difference between the corresponding temperature components in the considered region is insignificant for  $Kn = 10^{-4}$ . However, the difference between the components becomes substantial even for Knudsen numbers of the order of 0.01.

Taking condensation into account in the calculations leads to two effects:

the release of energy from latent condensation heat into the flow. Within the model under consideration, the binding energy is released into internal degrees of freedom of clusters of size  $g > 2$  (see reaction (1)), as well as into translational and internal degrees of freedom of monomers and dimers under triple recombination of monomers during reaction (4);

a natural decrease of monomers during the formation and growth of clusters in the flow.

In view of the above-discussed factors, the condensation process contributes to an

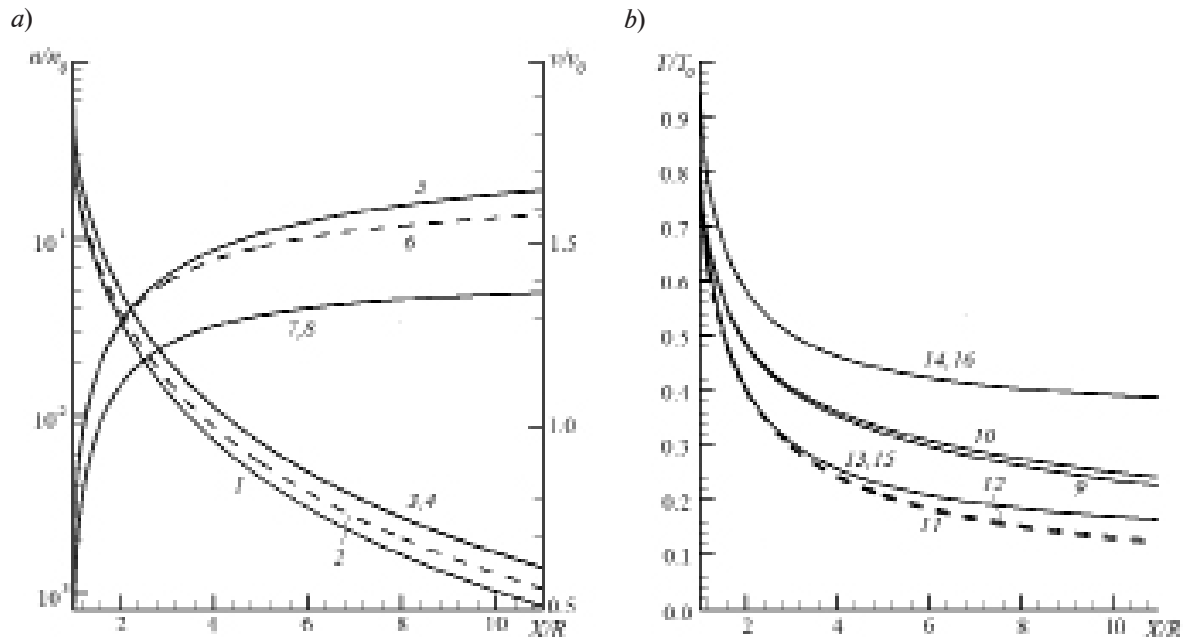


Fig. 1. Calculated density (curves 1 – 4) and velocity (5 – 8) distributions (a), and temperatures (b) of monomer vapor. Temperatures of translational (9, 11, 13, 15) and internal (10, 12, 14, 16) degrees of freedom are given. The calculations were performed with and without clustering taken into account (curves (1, 3, 5, 7, 9, 10, 13, 14) and (2, 4, 6, 8, 11, 12, 15, 16), respectively).  
 $Kn = 10^{-4}$  (1, 2, 5, 6, 9 – 12) and  $10^{-2}$  (3, 4, 7, 8, 13 – 16)

increase in the velocity and the temperature and to a faster decrease in the density of vapor in the flow. This effect can be clearly seen in Fig. 1 for the calculation variant ( $Kn = 10^{-4}$ ), for which the volume fraction of clusters is 5.4 %. The volume fraction of clusters in the flow for the Knudsen number 0.01 is less than 0.2 % and the condensation process has no effect on the gas dynamics of the flow.

The effect of clustering on the density and velocity distributions on the evaporating surface

is insignificant even for values of  $Kn = 10^{-4}$  (see Fig. 1). For example, the parameters of vapor on the sonic line differ by less than 3 % for the calculation variants with and without clustering taken into account (Table 2). The effect of the condensation process on the parameters of the sonic line turned out to be weaker compared with the results obtained in [19]. The distance of the sonic line from the evaporating surface in the variants with and without condensation is  $48.8\lambda_0$  and  $48.8\lambda_0$ , re-

Table 2

**Results of calculation of vapor parameters on the sonic line**

Variant number	Condensation taken into account	n/n <sub>0</sub>	T/T <sub>0</sub>	Reverse flow fraction, %
1	–	0.316	0.793	19.3
2	+	0.307	0.803	19.5

Note. The Knudsen number for the results given was  $Kn = 10^{-4}$ . The numbers of the variants correspond to those in Table 1.  
 Notations:  $n/n_0$  is the normalized concentration of vapor,  $T/T_0$  is the normalized temperature of vapor.

spectively (for  $Kn = 10^{-4}$ ). The effect of condensation on the flow parameters (especially on the temperature) increases with increasing distance from the surface.

A feature of this class of rarefied flows is its translational nonequilibrium, which increases with increasing Knudsen number. The regions of translational nonequilibrium (i.e., the regions where the components  $T_x$ ,  $T_\theta$ ,  $T_\phi$  of the translational temperature  $T_r$  are different) for any Knudsen number are found directly near the evaporating surface (a Knudsen layer with a thickness on the order of several mean free paths of molecules) and at some distance from the surface when the local mean free path of particles becomes large with respect to the characteristic flow size [18]. The data in Fig. 2, *a* show the dimensions of the Knudsen layer at the surface. The two following conditions have to be simultaneously fulfilled to determine the size of the layer [18, 19]:

$$\frac{|T_x - T_\theta|}{T} \cdot 100\% < 3\%;$$

$$\frac{|T_r - T_{int}|}{T} \cdot 100\% < 3\%,$$

where  $T_{int}$  is the temperature of the internal degrees of freedom

The resulting layer thickness is  $40\lambda_0$  and practically does not depend on taking into account the condensation process.

In case of collisionless expansion, the entire flow region is the zone of translational nonequilibrium [27]. The difference between the temperature components  $T_x$  and  $T_\theta = T_\phi$  is also observed in the larger flow region for the calculation variant with  $Kn = 10^{-2}$  (Fig. 2, *b*), and only in the far-field of the jet for the case  $Kn = 10^{-4}$ . As a result, taking into account the condensation process has no noticeable effect on the degree of flow nonequilibrium.

The presence of nonequilibrium regions (with respect to translational and internal degrees of freedom) argues in favor of choosing the kinetic approach as the calculation method, since it does not involve calculating the vapor temperature for determining the rates of the reactions under consideration.

A case in point is the calculation of the flow using the MCNT approach, with condensation taken into account. Fig. 3 shows the calculated data for the changes in the degree of

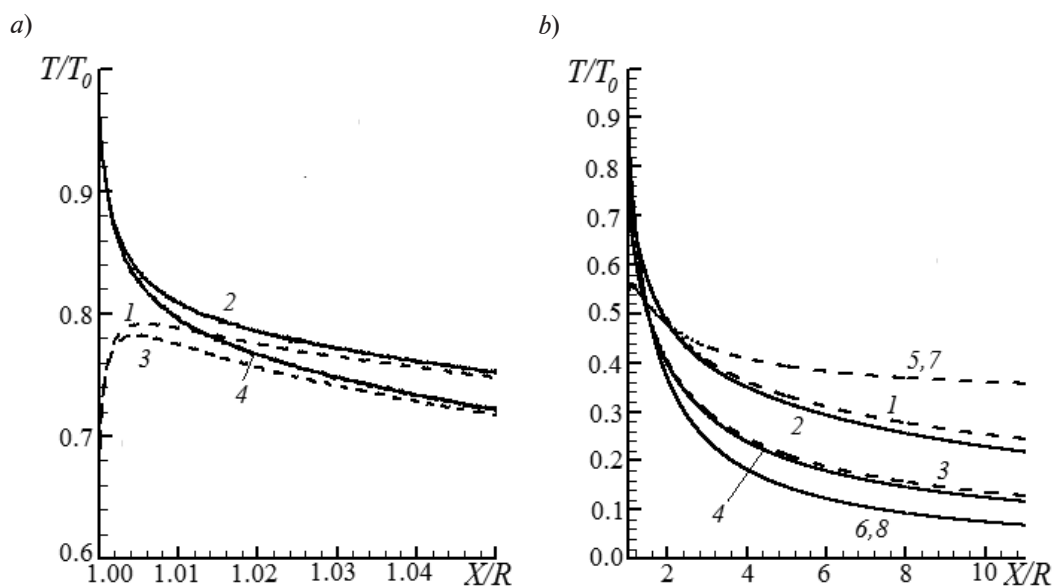


Fig. 2. Translational nonequilibrium near the surface of the sphere (*a*) and in the flow field (*b*). Data are given for the temperature components  $T_x$  (1, 3, 5, 7);  $T_\theta$ ,  $T_\phi$  (2, 4, 6, 8) at the values  $Kn = 10^{-4}$  (1 – 4) and  $10^{-2}$  (5 – 8). The calculations were carried out with (1, 2, 5, 6) and without (3, 4, 7, 8) clustering processes taken into account



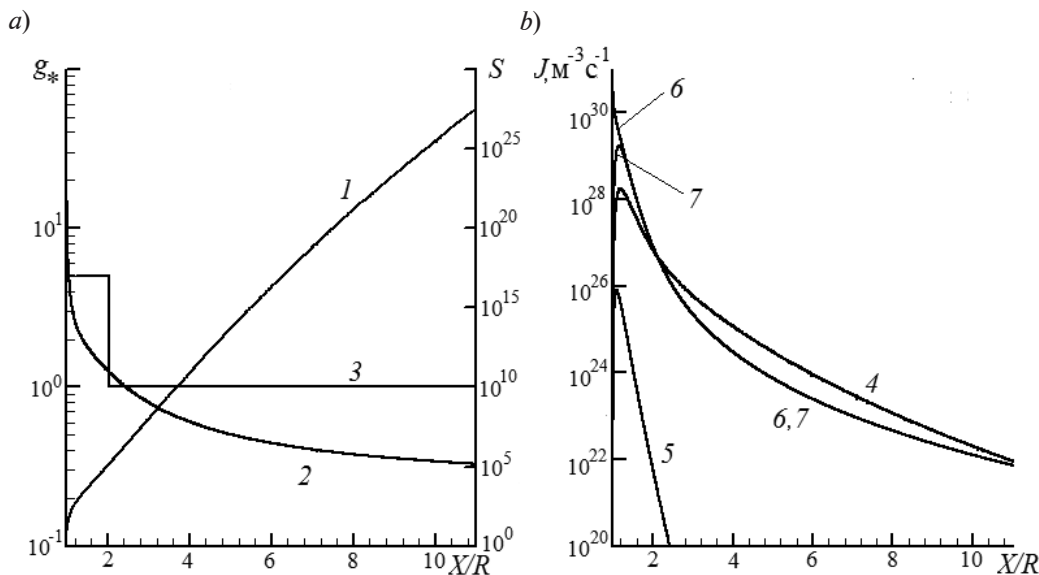


Fig. 3. Dependences of the supersaturation degree  $S$  (1), the critical cluster size  $g_*$  (2, 3) (a), the nucleation rates (4, 5, 7) and  $K_1$  (6) (b) versus the Knudsen numbers  $Kn = 10^{-4}$  (MCNT model). The values of  $g_*$  (curves 2 and 3 are the CNT and MCNT-based estimates, respectively),  $J_{clas}$  (4),  $J_K$  (5) and the calculated value of  $J$  (7) are given

supersaturation, the critical cluster size, and the nucleation rates as a function of the coordinate obtained for calculation variant 5 (the MCNT-based variant taking clustering into account, see Table 1). The degree of vapor supersaturation is small at the surface of the source where  $1.00 < X/R < 1.05$  (see Fig. 3,a), the size of the critical cluster  $g_* \gg 1$  and coincides for combined application of CNT and MCNT. The degree of supersaturation rapidly increases with distance from the source, and the critical size of the clusters decreases as a consequence. For this case, CNT predicts values of the degree of supersaturation to be less than unity as soon as distances of the order of one radius from the source are reached.

The MCNT approach predicts  $g_* = N_c$  at distances  $1.05 < X/R < 1.90$  (curve 3 in Fig. 3, a) from the source surface. The quantity  $g_*$  becomes equal to unity with further increase in the  $X/R$  coordinate.

The nucleation rates corresponding to the considered variants are shown in Fig. 3, b. The size of the critical cluster is fairly large directly at the surface of the source for low values of the equilibrium concentration  $n_{g^*}$ , predetermining low nucleation rates. The nucleation rate calculated by formula (1) for

MCNT coincides with the dimerization rate for triple collisions of monomers. The nucleation rate  $J_{clas}$ , calculated by the CNT formula [2], and the velocity  $J_K = J_{clas}/S$  with the Courtney correction differ significantly from the  $J$  values obtained within the MCNT model.

The behavior of clusters obtained by the calculation based on the kinetic approach is characterized by rather intense evaporation, and the maximum cluster size achieved in these calculations is limited to fourteen monomers. According to the calculations based on the MCNT, the clusters evaporate at a temperature equal to the translational temperature of the monomer vapor. The cluster growth rate turns out to be significantly higher than the evaporation rate. As a result, the number of clusters with the sizes  $g \gg 1$  varies little with increasing  $g$ .

Fig. 4 also shows the data for calculation variant 6 (see Table 1), where the injection of critical clusters into a cell was based on the MCNT model, and the evaporation in each cluster depended on its individual internal temperature (the same as with the kinetic approach). Apparently, using this approach brings the results substantially closer to those obtained based on the kinetic model.

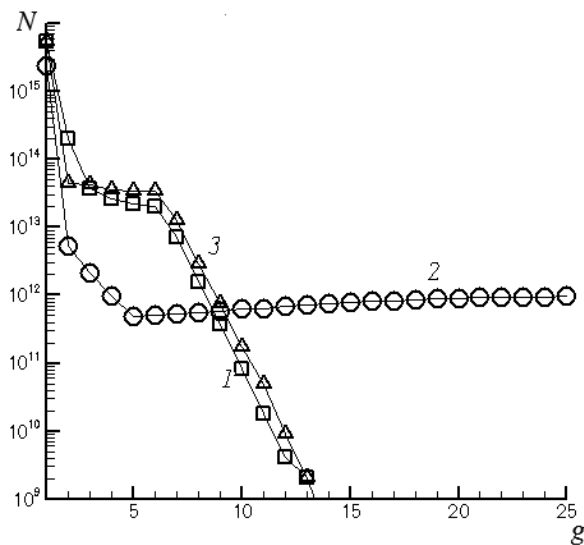


Fig. 4. Size distributions of clusters in the flow field, obtained from the calculation variants 2 (curve 1), 5 (2) and 6 (3)

The coordinate distributions of the density and the mole fraction of the clusters are shown in Fig. 5 for the Knudsen number  $10^{-4}$ . Dimers ( $g = 2$ ) form in the immediate vicinity of the source surface. The peaks on the distributions 5-mers ( $g = 5$ ) are shifted away from

the surface. The distance from the distribution maximum to the source increases with increasing cluster size. Fig. 5, *b* shows the coordinate distributions of the mole fraction of the clusters with the sizes  $g = 2, 3$  and 5. The presented results indicate freezing of the mole fractions starting with a certain coordinate depending on the cluster size. Since the nucleation rate  $J$  is low near the source, the dimer concentrations at the surface, obtained by direct statistical simulation based on MCNT, are small compared to the concentrations obtained based on the kinetic approach, and the maximum of the dimer distribution is shifted away from the surface by  $0.25R$ .

The concentrations of the 5-mers in the greater part of the flow turn out to be substantially smaller than similar concentrations obtained using the kinetic approach. In case of variant 6 (MCNT model, with evaporation considered in accordance with the kinetic approach), the distributions of dimer and 5-mer concentrations turn out to be closer to the results of the calculations based on the kinetic approach (variant 5), however, the data do not coincide.

We should note that the results obtained

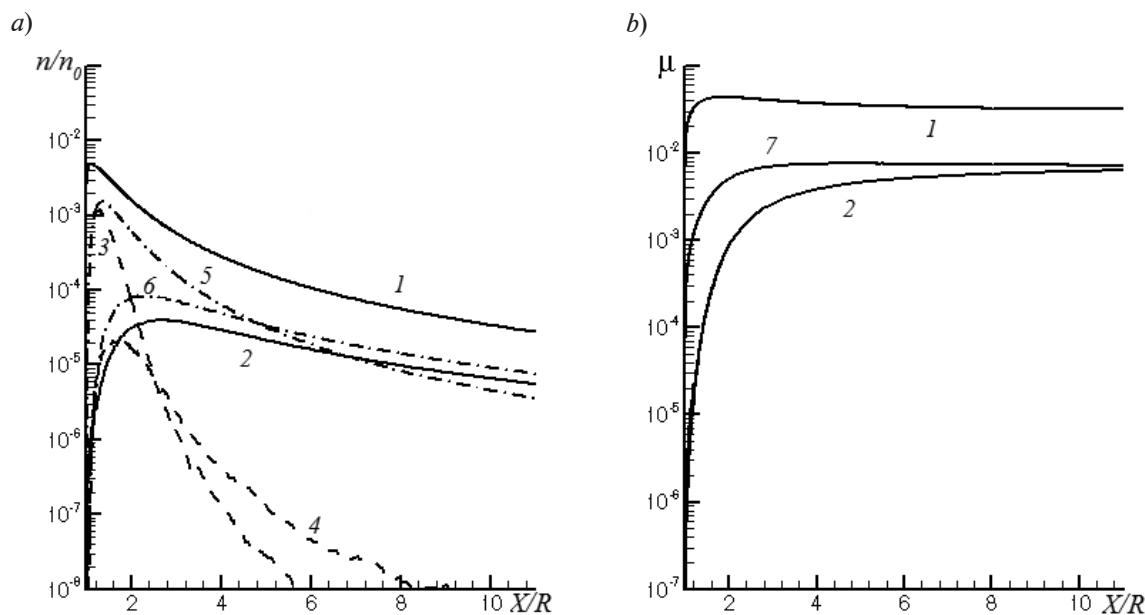


Fig. 5. Distributions of concentration (a) and mole fraction (b) of clusters along the radial coordinate for clusters with different sizes  $g$ . The calculations are based on the kinetic approach (1, 2, 7), on MCNT (3, 4) and on variant 6 (5, 6);  $g = 2$  (1, 3, 5), 3 (7) and 5 (2, 4, 6). Knudsen number  $Kn = 10^{-4}$

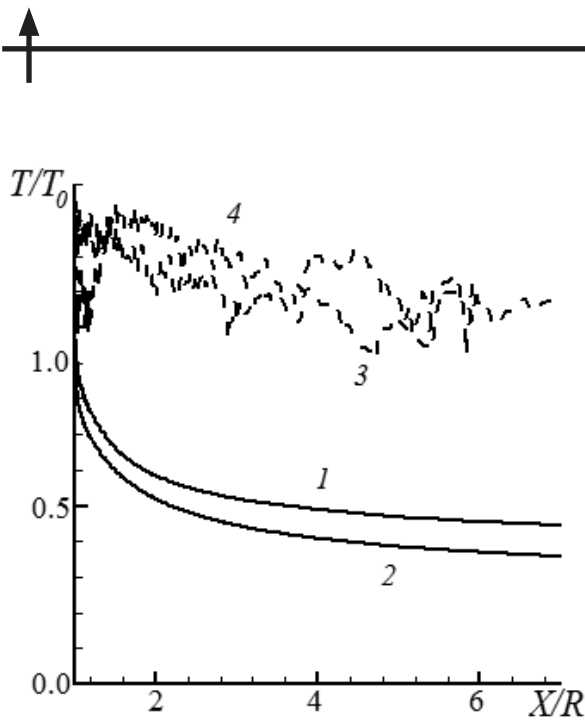


Fig. 6. Distributions of the internal temperature of particles along the radial coordinate for clusters of two sizes: dimers (curves 1, 3) and trimers (2, 4). Calculations are based on the kinetic approach (1, 2) and on MCNT (3, 4)

using the model [11] differ from those in [19]. Size distributions of clusters have a maximum corresponding to the dimer size.

The translational velocities of the growing clusters coincide with the monomer velocity for the calculation variant with  $Kn = 10^{-4}$ . The internal temperatures of the clusters are shown in Fig. 6. These temperatures of dimers and trimers are above the translational temperature because latent condensation heat is released into the flow during cluster growth. The growth is accompanied by evaporation of clusters, during which the binding energy is absorbed. The evaporation rate of each cluster within the model based on the kinetic approach depends on its own internal temperature and this rate proves to be comparable with the growth rate. As a result, the evaporation process leads to a moderate difference in the translational and internal temperatures of the clusters and a limited maximum cluster size (see Fig. 4). The evaporation rate for the MCNT model is governed by the translational temperature of the monomers. The growth process plays the principal role within the MCNT-based approach. The evaporation of clusters, which reduces their

internal energy, has a rate that is small compared to their growth rate. As a result, growth of large clusters ( $g \gg 1$ ) is observed, and the energy that is released during this process is accumulated in internal degrees of freedom. The internal temperature of the clusters obtained in the calculations based on the MCNT model is higher than the internal temperatures of the clusters predicted by the kinetic model of condensation (see Fig. 6).

### Conclusion

We have carried out a calculation of expansion of water vapor into vacuum from the surface of a spherical source by direct statistical modeling, taking into account cluster growth in the flow field. Two models of the clustering process were used for the calculations:

one based on the conclusions of the modified classical nucleation theory;

and one based on the kinetic approach.

One of the main drawbacks of MCNT is that the model based on it is single-temperature. It is impossible to correctly describe the processes of evaporation of monomers from clusters within this approach. Implementing the model through a computational algorithm is complex and additional assumptions have to be introduced. The calculated main characteristics of clustering (the spatial distribution of the cluster concentration, the size distribution of clusters in the flow field) obtained using the MCNT model differ significantly from those obtained by the model based on the kinetic approach.

The kinetic model is free of all drawbacks of the MCNT model. This approach allows to obtain the probabilities of cluster growth/evaporation as functions of individual parameters of colliding/decaying particles, which is in full agreement with the DSMC method. The temperature of vapor in a cell does not need to be determined for simulating the condensation process. From a methodological standpoint, using a model based on the kinetic approach is justified.

Calculations of condensation of water vapor expanding from a spherical surface into vacuum based on the kinetic model in near-continuous and transient Knudsen regimes indicate that the condensation process does not

affect the parameters of gas-dynamic flow at clustering degrees less than 1 %. The degree of clustering becomes noticeable (5.4 %) in near-continuous regimes ( $Kn = 10^{-4}$ ). In this case, the release of latent heat of condensation into the flow leads to a faster growth of gas velocity and temperature and to a drop in gas density. The clustering process has a particularly strong effect on the distribution of translational and internal temperatures of the vapor. However, even for the calculation variant corresponding to  $Kn = 10^{-4}$ , the condensation process does not significantly affect the parameters of the sonic line, the size of the Knudsen layer, and the degree of translational nonequilibrium compared to the calculation results obtained

without taking into account the condensation process. The maximal concentration of clusters in the flow field corresponds to size of a dimer.

The study has described the effect of the mole fractions of clusters ‘freezing’ as they move away from the surface of the source. For larger clusters, the effect is observed at large distances from the evaporated surface. The rates and translational temperatures of the clusters formed in the flow prove to be close to the corresponding parameters of the monomers. The release of binding energy in the process of particle association leads to higher values of internal temperatures of the clusters compared to the internal temperature of the monomers.

#### REFERENCES

- [1] **J.F. Crifo**, Water clusters in the coma of comet Halley and their effect on the gas density, temperature, and velocity, *Icarus*. 84 (2) (1990) 414–446.
- [2] **L.E. Sternin**, *Osnovy gazodinamiki dvukhfaznykh techeniy v soplakh* [Fundamentals of gas dynamics of two-phase flows in the nozzles]. Mashinostroyeniye, Moscow, 1974.
- [3] **Yu.V. Platov, B.P. Filippov, A.I. Semenov**, Condensation of combustion products in the exhaust plumes of rocket engines in the upper atmosphere, *Geomagnetism and Aeronomy*. 51 (4) (2011) 550–556.
- [4] **G.A. Bird**, *Molecular gas dynamics and the direct simulation of gas flows*, Clarenton Press, Oxford, 1994.
- [5] **B. Briehe, H.M. Urbassek**, Monte Carlo simulation of growth and decay processes in a cluster aggregation source, *J. Vac. Sci. Technol. A*. 17 (1) (1999) 256–265.
- [6] **M.I. Zeifman, B.J. Garrison, L.V. Zhigilei**, Combined molecular dynamics direct simulation Monte Carlo computation study of laser ablation plume evolution, *J. Appl. Phys.* 92 (4) (2002) 2181–2193.
- [7] **N.Yu. Bykov, G.A. Lukyanov**, Direct simulation Monte Carlo of pulsed laser ablation of metals with clusterization processes in vapor, *Thermophysics and Aeromechanics*. 13 (4) (2006) 569–582.
- [8] **T.E. Itina, K. Gouriet, L.V. Zhigilei, et al.**, Mechanisms of small clusters production by short and ultra-short pulse laser ablation, *Appl. Surf. Sci.* 253 (19) (2007) 7656–7661.
- [9] **Z. Li, J. Zhong, D.A. Levin, B.J. Garrison**, Development of homogeneous water condensation models using molecular dynamics, *AIAA Journal*. 47 (5) (2009) 1241–1251.
- [10] **R. Jansen, I. Wysong, S. Gimelshein, et al.**, Nonequilibrium numerical model of homogeneous condensation in argon and water vapor expansions, *J. Chem. Phys.* 132 (24) (2010) 244105.
- [11] **N.Yu. Bykov, Yu.E. Gorbachev**, Mathematical models of water nucleation process for the Direct Simulation Monte Carlo method, *Applied Mathematics and Computation*. 296 (1 March) (2017) 215–232.
- [12] **J. Zhong, M.I. Zeifman, S.F. Gimelshein, D.A. Levin**, Modeling of homogeneous condensation in supersonic plumes with the DSMC method, *AIAA Paper* (2004), 42<sup>nd</sup> Aerospace Sciences Meeting, Jan. 5 – 8, Reno, Nevada, 2004-0166.
- [13] **J. Zhong, M.I. Zeifman, S.F. Gimelshein, D.A. Levin**, Direct simulation Monte Carlo modeling of homogeneous condensation in supersonic plumes, *AIAA Journal*. 43 (8) (2005) 1784–1796.
- [14] **N.Y. Bykov, Y.E. Gorbachev**, Direct statistical simulation of the processes of clusters formation in the gas phase: classical approach with cluster size correction, *High Temperature*. 53 (2) (2015) 291–300.
- [15] **D.I. Zhukhovitskii**, Size-corrected theory of homogeneous nucleation, *J. Chem. Phys.* 101 (6) (1994) 5076–5080.
- [16] **N.Y. Bykov, Y.E. Gorbachev**, Comparative analysis of condensation models within DSMC, *AIP Conference Proceedings*. 1628 (1) (2014) 139–147.
- [17] **N.M. Bulgakova, M.Yu. Plotnikov, A.K. Rebrov**, Modeling steady-state gas expansion from a spherical surface into a vacuum, *Fluid Dynamics*. 32 (6) (1997) 137–143.
- [18] **G.A. Lukyanov, Gr.O. Khanlarov**, Stationary water vapor expansion from a spherical surface into vacuum, *Thermophysics and Aeromechanics*. 7 (4) (2000) 511–521.



- [19] **N.Yu. Bykov**, Modelling of condensation at spherical expansion of water vapor into vacuum, *Thermophysics and Aeromechanics*. 2009. 16 (2) (2009) 189–199.
- [20] **G.A. Bird**, Simulation of multi-dimensional and chemically reacting flows, In: *Rarefied Gas Dynamics*, ed. by R. Campargue, Commissariat a Lenergie Atomique, Paris, 1 (1979) 365–388.
- [21] **S.F. Gimelshein, N.E. Gimelshein, D.A. Levin, et al.**, On the use of chemical reaction rates with discrete internal energies in the direct simulation Monte Carlo method, *Physics of Fluids*. 16 (7) (2004) 2442–2451.
- [22] **N. Goldman, R.S. Fellers, C. Leforestier, R.J. Saykally**, Water dimers in the atmosphere: Equilibrium constant for water dimerization from the VRT (ASP-W) potential surface, *J. Phys. Chem. A*. 105 (3) (2001) 515–519.
- [23] **J. Wolk, R. Strey**, Homogeneous nucleation of H<sub>2</sub>O and D<sub>2</sub>O in comparison: the isotope effect, *J. Phys. Chem. B*. 105 (47) (2005) 11683–11701.
- [24] **X. Xu, W. Goddard**, Bonding properties of water dimer: a comparative study of density functional theories, *J. Phys. Chem. A*. 108 (12) (2004) 2305–2313.
- [25] **N.Y. Bykov, Y.E. Gorbachev, V.V. Zakharov**, Simulation of small cluster formation in water vapor plumes, *AIP Conference Proceedings*, 1786 (1) (2016) 050001-1–050001-8.
- [26] **G.G. Cherniy**, *Gazovaya dinamika [Gas dynamics]*, Nauka, Moscow, 1988.
- [27] **Yu.A. Koshmarov, Yu.A. Ryzhov**, *Prikladnaya dinamika razrezhennogo gaza [Applied rarefied gas dynamics]*, Mashinostroyeniye, Moscow, 1977.

*Received 30.11.2017, accepted 08.02.2018.*

#### THE AUTHOR

**BYKOV Nikolay Yu.**

*Peter the Great St. Petersburg Polytechnic University*

29 Politechnicheskaya St., St. Petersburg, 195251, Russian Federation

nbykov2006@yandex.ru